Supporting Information for

Moiety-Specific Mechanism of ATP's Hydrotropic Action on α-Synuclein

Yusuke Shuto,[a] Toshifumi Mori,[bc†] Benjamin Kohn,[d‡] Erik Walinda,[e] Daichi Morimoto,[f] Ulrich Scheler,[d] Masatomo So,[a] Ayako Furukawa,[a] Norio Yoshida[g] and Kenji Sugase[a*]

[a] Division of Applied Life Sciences, Graduate School of Agriculture, Kyoto University, Kitashirakawa Oiwake-cho, Sakyo-ku, Kyoto 606-8502, Japan

[b] Institute for Materials Chemistry and Engineering, Kyushu University, Kasuga, Fukuoka 816-8580, Japan

[c] Department of Interdisciplinary Engineering Sciences, Interdisciplinary Graduate School of Engineering Sciences, Kyushu University, Kasuga, Fukuoka 816-8580, Japan

[d] Leibniz-Institut für Polymerforschung Dresden e.V., Hohe Str. 6, 01069 Dresden, Germany

[e] Department of Molecular and Cellular Physiology, Graduate School of Medicine, Kyoto University, Yoshida Konoe-cho, Sakyo-ku, Kyoto 606-8501, Japan

[f] Department of Molecular Engineering, Graduate School of Engineering, Kyoto University, Nishikyo-ku, Kyoto 615-8510, Japan

[g] Graduate School of Informatics, Nagoya University, Furo-cho, Chikusa-ku, Nagoya 464-8601, Japan

[†] Current address: Department of Molecular Engineering, Graduate School of Engineering, Kyoto University, Nishikyo-ku, Kyoto 615-8510, Japan

[‡] Current address: Department of Radiology, Washington University in Saint Louis, St. Louis, MO 63110, United States

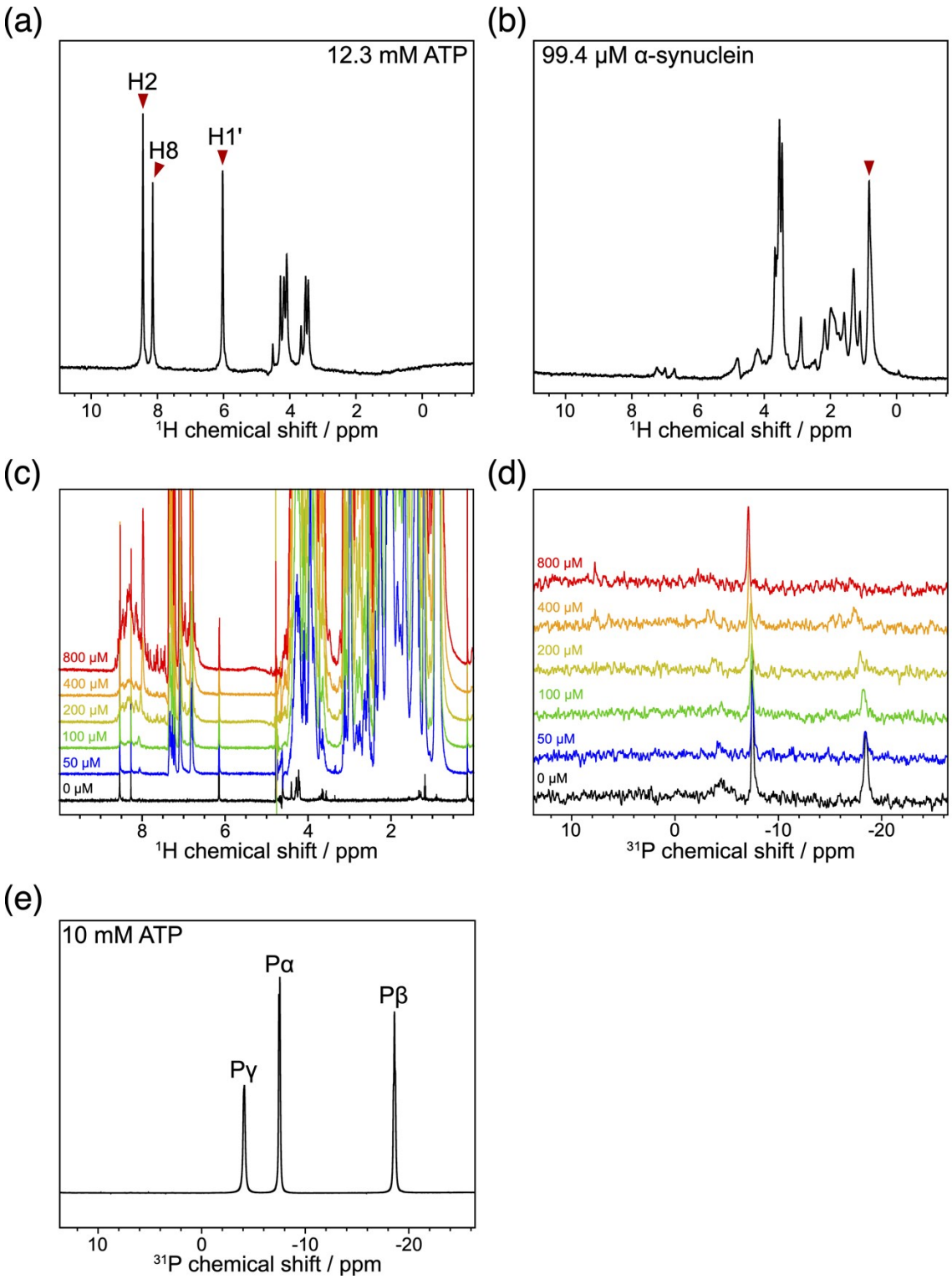

Fig. S1 ^{1}H NMR spectra of (a) 12.3 mM ATP, (b) 99.4 µM α-synuclein, and (c) 100 µM ATP in the presence of increasing α-synuclein concentrations. ^{31}P NMR spectra of (d) 100 µM ATP in the presence of increasing α-synuclein concentrations and (e) 10 mM ATP. No ^{31}P NMR signal

corresponding to free phosphate was detected, indicating the absence of ATP degradation.

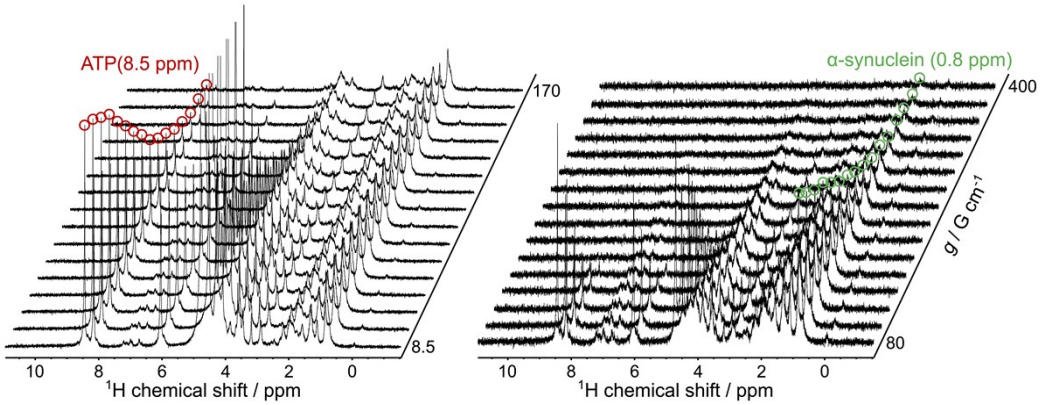

Fig. S2 Diffusion NMR measurements of a solution containing 99.4 µM α-synuclein and 12.3 mM ATP in D_2O. Different gradient strengths were applied for each component within the same sample: 8.5–170 G cm^{-1} for ATP (left) and 80–400 G cm^{-1} for α-synuclein (right). Analyzed signals are marked with red circles for ATP and green circles for α-synuclein.

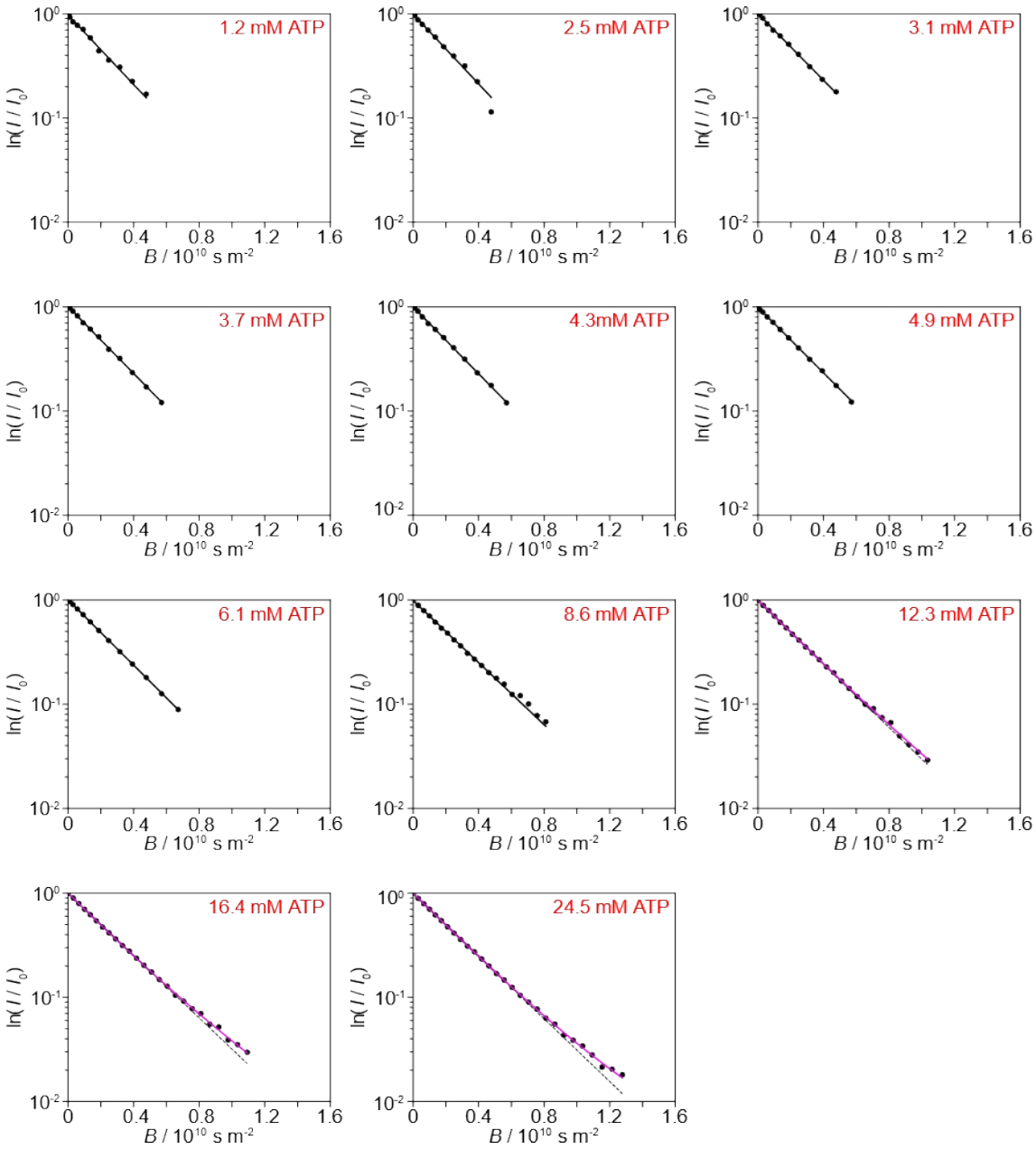

Fig. S3 Diffusion measurements of ATP in the absence of α-synuclein. The ATP signal at 8.5 ppm was analyzed. Normalized signal intensity (log scale) is plotted against *B* values in Stejskal-Tanner plots. The dots, black solid lines, black dashed lines, and magenta lines represent the experimental values, single-component fits, extrapolations of the single-component fits, and two-component fits, respectively. Data points with signal intensities at or near the noise level were excluded from the fitting. At lower ATP concentrations, fewer points were included due to reduced sensitivity.

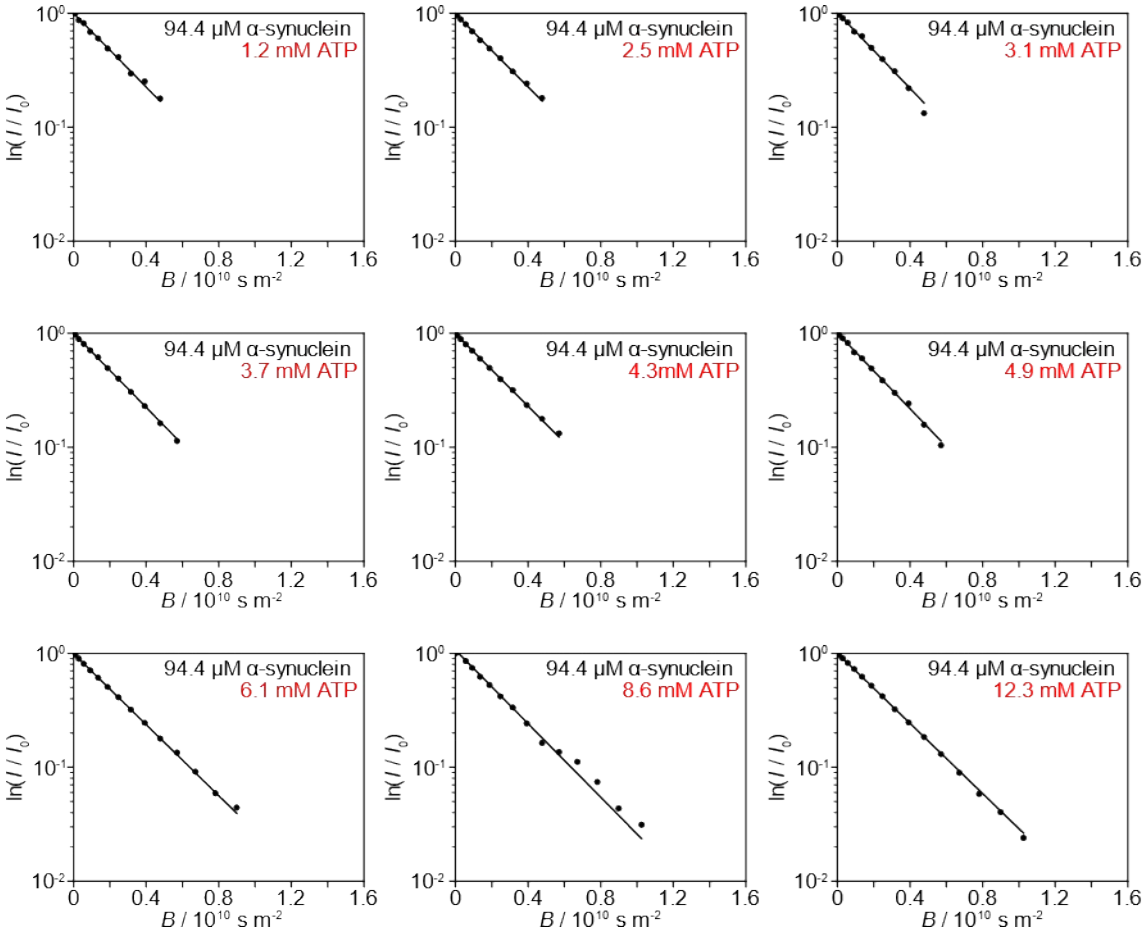

Fig. S4 Diffusion measurements of ATP in the presence of α-synuclein. The ATP signal at 8.5 ppm was analyzed. Normalized signal intensity (log scale) is plotted against *B* values in Stejskal-Tanner plots. The dots and black solid lines represent the experimental values and single-component fits, respectively. Data points with signal intensities at or near the noise level were excluded from the fitting. At lower ATP concentrations, fewer points were included due to reduced sensitivity.

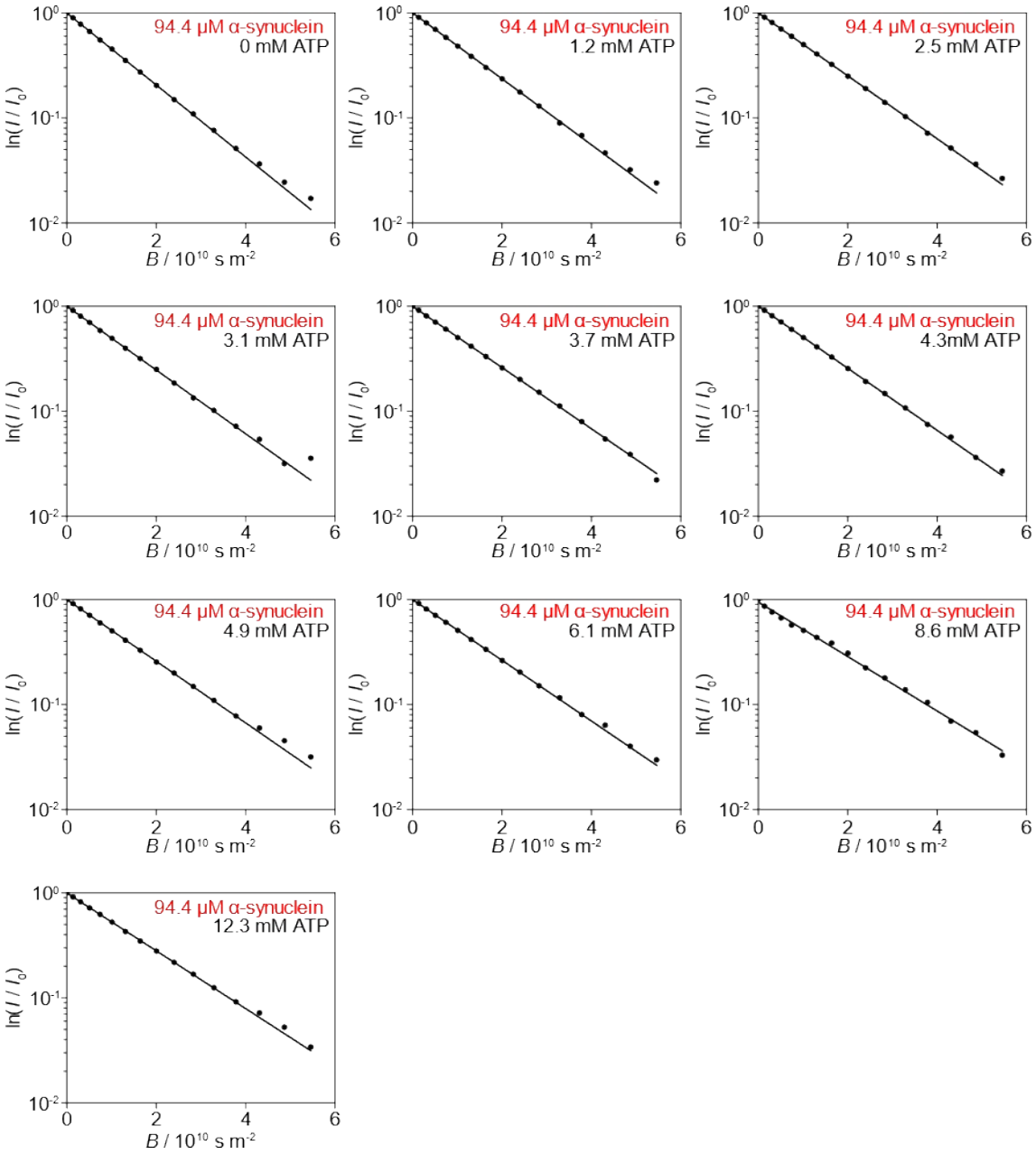

Fig. S5 Diffusion measurements of α-synuclein in the presence of ATP. The α-synuclein signal at 0.8 ppm was analyzed. Normalized signal intensity (log scale) is plotted against *B* values in Stejskal-Tanner plots. The dots and black solid lines represent the experimental values and single-component fits, respectively.

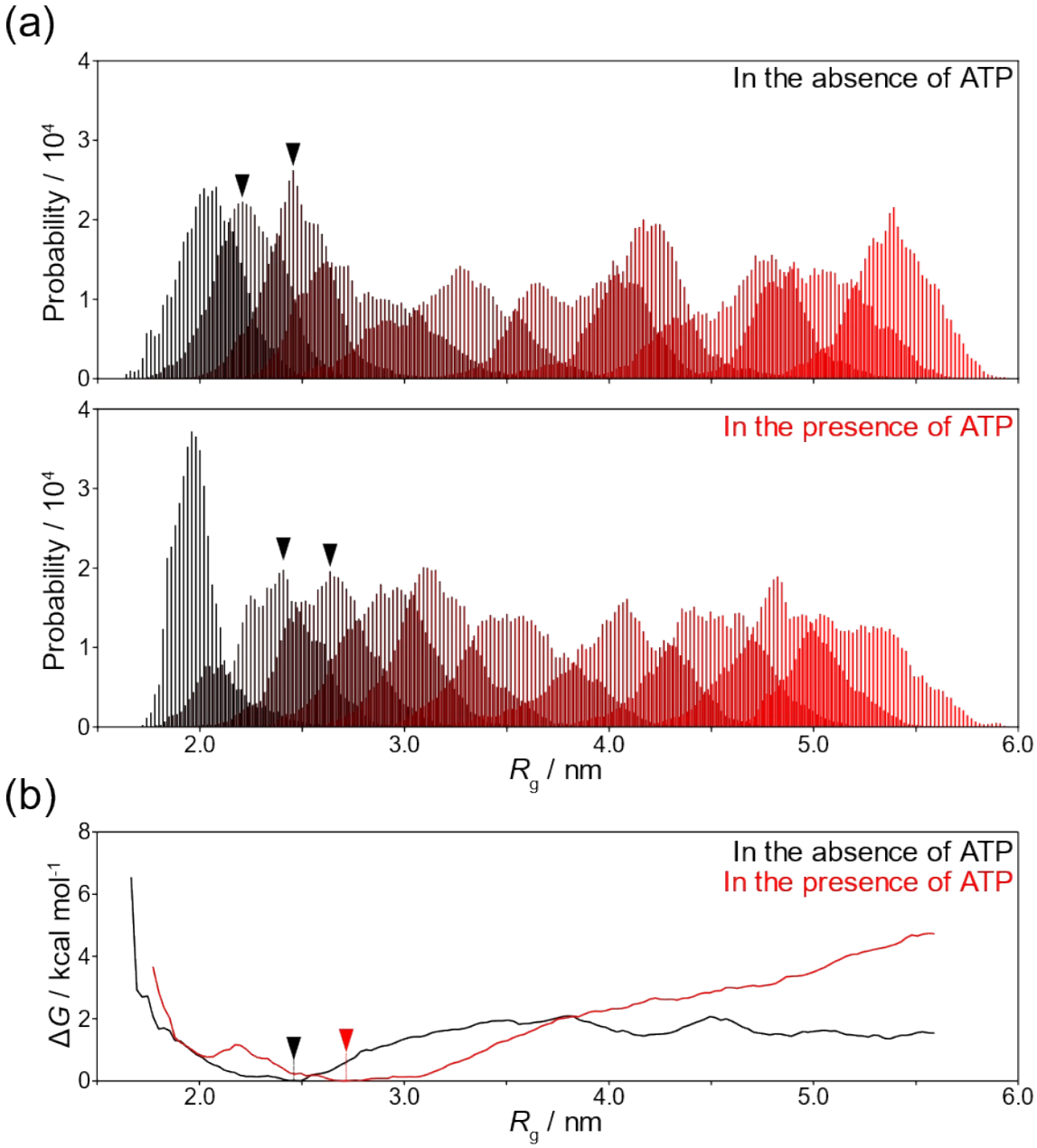

Fig. S6 (a) R_g distributions of α-synuclein from MD simulations without (top) and with (bottom) ATP. Histograms of ten replicas are colored in a gradient from black to red. The replicas marked with black triangles at their peaks were selected for further analyses. (b) Free energy profiles as a function of R_g in the absence (black) and presence (red) of ATP. The free energy profiles were shifted to set the minimum value to zero. Black and red triangles indicate R_g values at the global free energy minima in the absence and presence of ATP, respectively.

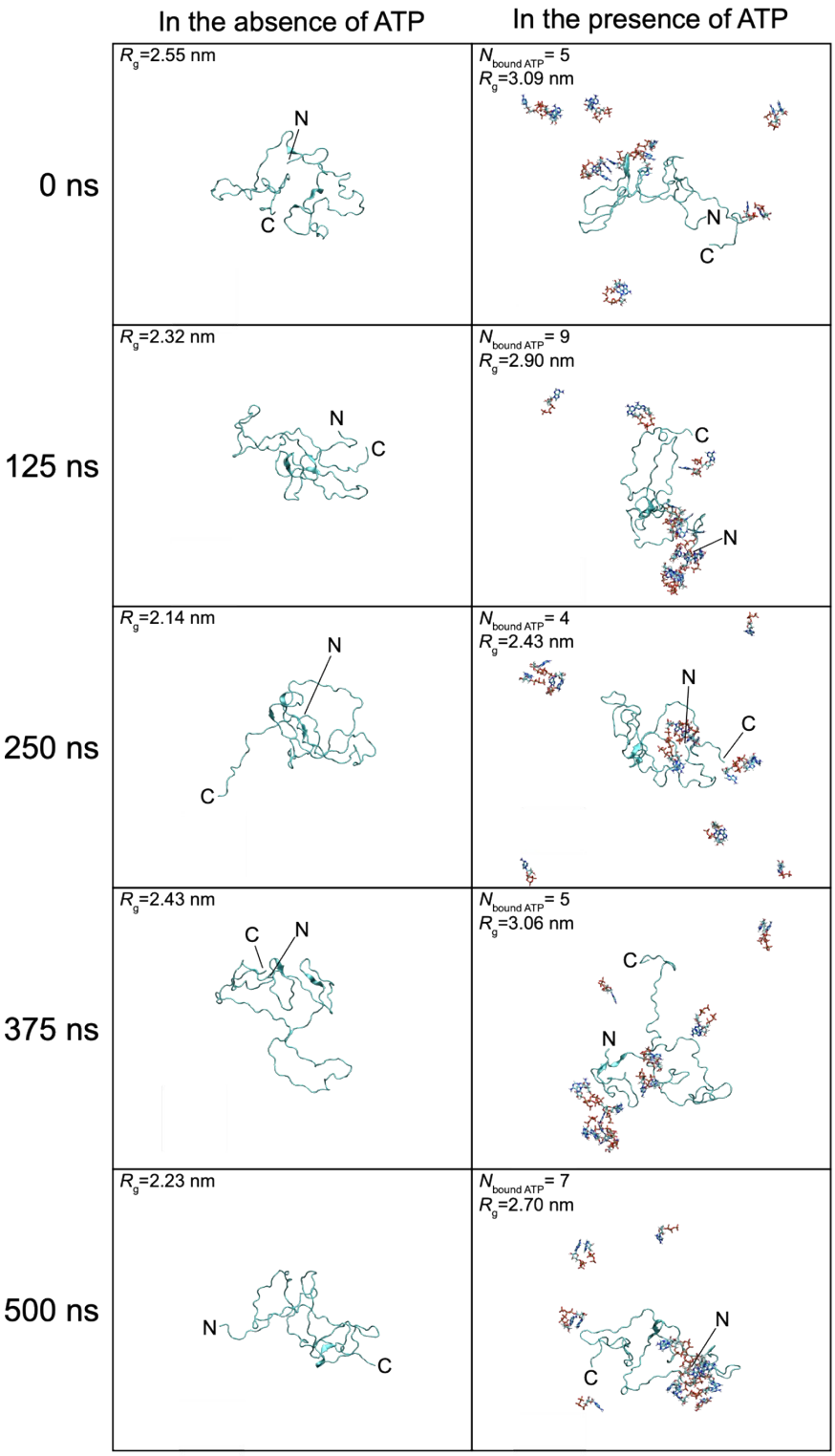

Fig. S7 Representative α-synuclein structures in the absence (upper) and presence (lower) of ATP at simulation times of 0, 125, 250, 375, and 500 ns. α-Synuclein is depicted as a cyan cartoon, and ATP molecules are shown in licorice representation. R_g and the number of binding ATP are shown at the upper left of each snapshot.

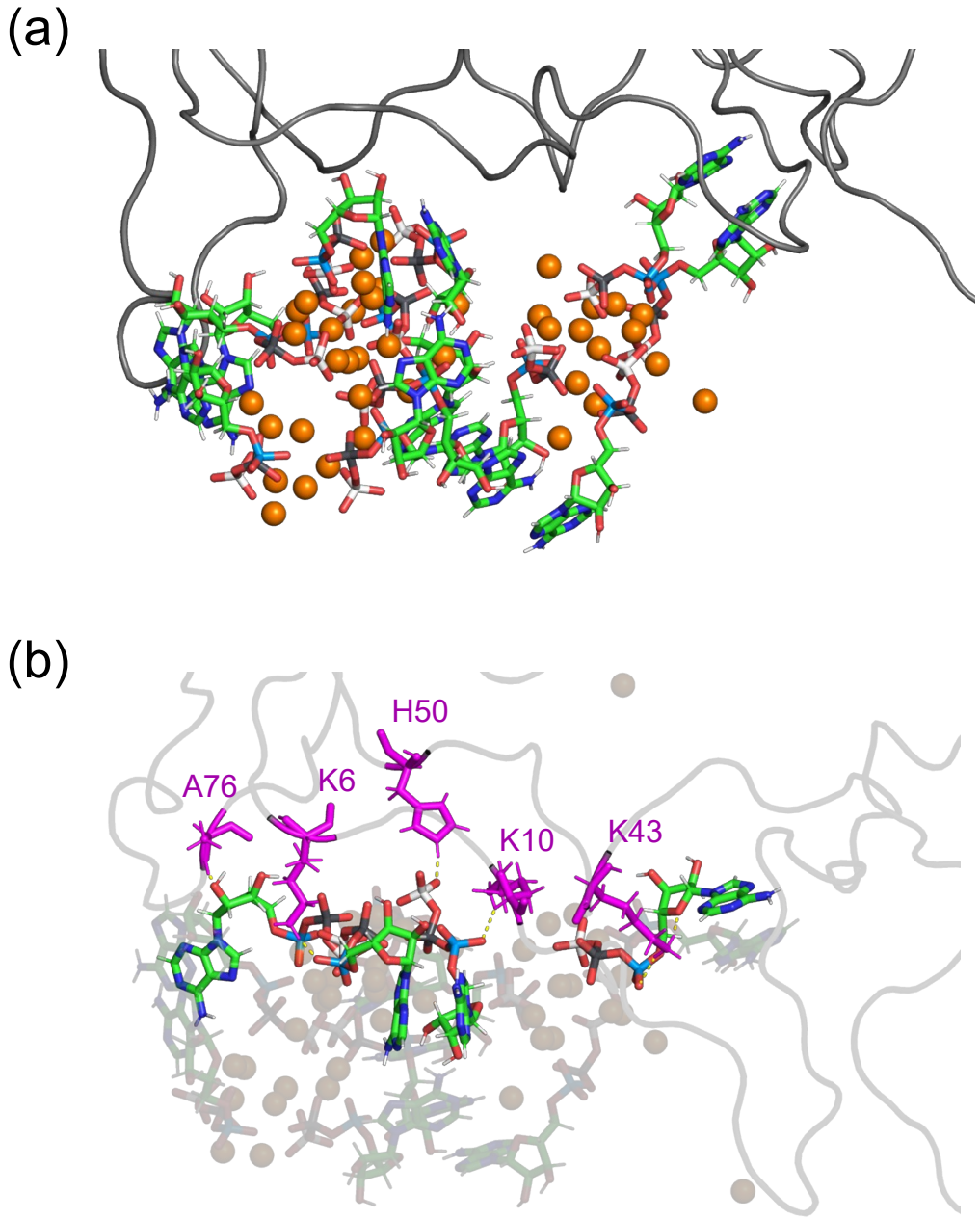

Fig. S8 (a) Representative α-synuclein structure in the presence of ATP and sodium ions in the final snapshot of the simulation. α-Synuclein is depicted as a grey cartoon, ATP molecules are shown in licorice representation, and sodium ions are shown as orange spheres. (b) Intermolecular hydrogen bonds highlighted between α-synuclein and ATP in the same frame shown in (a). Yellow dashed lines indicate hydrogen bonds, and magenta stick models represent amino acid residues involved in the hydrogen bonds.

Table S1. Hydrodynamic radii of ATP and its populations calculated by a two-component fit.

ATP concentration / mM	First component		Second component	
	Population	R_h / nm	Population	R_h / nm
12.3	0.71 ± 0.61	0.42 ± 0.11	0.28 ± 0.61	0.65 ± 0.21
16.4	0.89 ± 0.15	0.44 ± 0.04	0.11 ± 0.15	0.79 ± 0.26
24.5	0.98 ± 0.02	0.48 ± 0.01	0.02 ± 0.02	1.24 ± 0.46